Materials International
Open Access Journal (ISSN: 2668-5728)

Article
Volume 6, Issue 2, 2024, 12
https://doi.org/10.33263/Materials62.012

Sodium Citrate as a Corrosion Inhibitor for Carbon Steel

Lucas Silva [1], Amauri Souza [1], Cristiane Taroco [2], Eric Garcia [1], Gabriel Santos [1], Julio Onésio Melo [1], Talita Dias [1], Tulio Matencio [3], Hosane Taroco [1,*]

1. Departamento de Ciências Exatas e Biológicas, Universidade Federal de São João del-Rei, Sete Lagoas, MG, Brazil
2. Departamento de Engenharia Elétrica, Universidade Federal de São João del-Rei, São João del-Rei, MG, Brazil
3. Departamento de Química, Universidade Federal de Minas Gerais, Belo Horizonte, MG, Brazil

* Correspondence: hataroco@ufsj edu.br;

Scopus Author ID 33667954900

Received: 28.09.2023; Accepted: 28.01.2024; Published: 10.06.2024

Abstract: In this paper, sodium citrate was used as a corrosion inhibitor for carbon steel in a 125 ppm of chloride solution at pH= 6 to simulate a typical cooling water. In both cases, on the anodic and cathodic side, the presence of the inhibitor caused an increase in the Tafel coefficient, possibly due to the change in the alpha value. According to adsorption measurements, the corrosion inhibition by citrate can be characterized as a mixture of chemisorption and physisorption. Thermodynamic values for the activated complex also indicate a mixed mechanism. Furthermore, the increased free Gibbs energy for activating complex value shows that the corrosion process is less spontaneous when using sodium citrate as a corrosion inhibitor. Through XRD measurements for a steel sample immersed in the citrate solution, there is a clear reduction in the intensity of the peaks in the diffractogram due to the smaller amount of corrosion product formed. Furthermore, EDX and SEM measurements corroborate the formation of a thin inhibitor layer on the steel.

Keywords: sodium citrate; corrosion inhibition; adsorption; carbon steel.

1. Introduction

In the industrial, the process of pasteurization requires a large amount of water, with an efficient temperature control system. There is a range of materials available for industrial piping; however, carbon steel alloys are the main ones used due to their variety of applications and advantageous properties [1-11]. Despite being widely used, most carbon steel cannot resist corrosion in the environment where it is used, where it naturally tends to deteriorate. Therefore, strategies must be used to mitigate corrosion. In this sense, corrosion inhibitors can be applied to practically any cooling system. The search for natural and biodegradable compounds plays a satisfactory role in corrosion inhibition [1-5]. Thus, studying citric acid or sodium citrate becomes very promising [7, 12-21]. In the food and beverage industry, citric acid is mainly used due to its antioxidant properties, which are used to preserve food or as an acidifier [7,12-21].

According to the literature, adding sodium citrate increases corrosion due to the displacement of Fe^{+2} ions from the passive layer [22]. In this proposal, the corrosion mechanism is accentuated by the adsorption of citrate ions [22]. However, when using chlorides, pitting corrosion is partially blocked by the presence of sodium citrate [23]. In this mechanism, the diffusion of complexed Fe^{+2} ions is smaller than its metal aquo complex. In this way, diffusion limits corrosion, which decreases the corrosion rate (CR) [23]. Ashassi et

al. [24] showed that diffusion using a rotating electrode strongly influences sodium citrate's anticorrosive effect. However, from a rotation of 2000 rpm, there is a decrease in the inhibition promoted by sodium citrate [24].

Thus, in this work, the electrochemical corrosion of carbon steel in an aqueous medium with 125 ppm chloride and pH = 6.00 simulates a typical cooling water. Furthermore, the effect of sodium citrate as a corrosion inhibitor was studied.

2. Materials and Methods

In this study, a cell with three electrodes was used. The auxiliary electrode consisted of Pt (4 cm^2). The reference electrode was the saturated Ag/AgCl, and the working electrode was carbon steel. The working electrode was sanded with 1500 water sandpaper, washed with deionized water and alcoholic solution, and dried at room temperature. The exposed area of the electrode for linear polarization analysis was 1 cm^2. The linear polarization measurements were performed on an Autolab PGSTAT potentiostat. The curves were treated using the NOVA©68 software, where the linearization of the anodic and cathodic curves was performed, around ± 30 mV in relation to open circuit potential (OCP), and the potential scan rate used was 0.16 mVs^{-1}. The electrolyte was prepared with the addition of 125 ppm of NaCl adjusted with pH = 6.00 with a stock solution of clorhidric acid $1x10^{-3}$M. The corrosion inhibitor tri-sodium citrate (Na_3Cit) dehydrate (Sigma-Aldrich) was added at different concentrations to study its effect as a corrosion inhibitor. The corrosion rate was calculated using the Faraday Law (Equation 1), and the coverage degree was calculated using Equation 2. To study the effect of temperature on steel corrosion with and without Na_3Cit, the electrochemical cell was kept in a thermostatic water bath (Láctea cientifica LAC – F30/CD) in temperatures 288, 298, and 308 K.

$$CR = \frac{MM.i_{corr}}{zF\rho} \qquad (Eq.1)$$

$$\theta = \frac{i_{corr} - i^{c}_{corr}}{i_{corr}} \qquad (Eq.2)$$

Where: i^{c}_{corr}, i_{corr} are corrosion currents: with and without Na_3Cit, respectively; θ is the coverage degree; Z is the electric charge of the ion; F is the Faraday's constant (96500 C /mol); and ρ is the metal density.

The XRD analyses were obtained by measures in the Shimadzu XRD-6000 diffractometer, operating in current scan mode (20º-70º), with Cu Kα radiation (λ = 1.54086 Å), generated at 30 kV and with 30 mA, with steps of $1ºs^{-1}$. SEM analyses were performed at the UFMG microscopy center. Micrographs were fitted on a Bruker Nano Berlin, Germany microscope with a secondary electron detector, backscattered, and EED with high vacuum mode operating between 10^{-6} and 10^{-7} torr and low vacuum mode operating at 10^{-2} torr.

3. Results and Discussion

Figure 1 shows the corrosion rate behavior of carbon steel in different sodium citrate (Na_3Cit) concentrations.

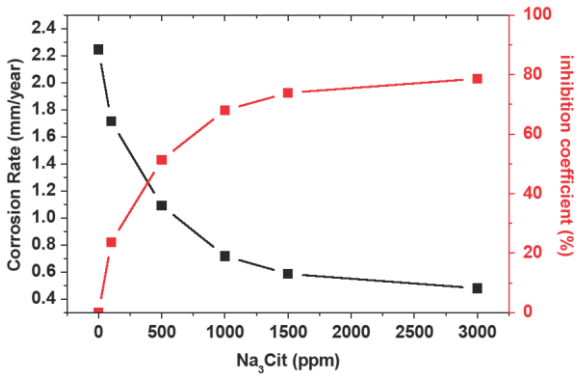

Figure 1. Corrosion rate behavior of carbon steel in different sodium citrate (Na_3Cit) concentrations in pH = 6.00 and 125ppm of chloride.

The Na_3Cit promotes a reduction of around 80% of corrosion rate. The corrosion inhibition effect promoted by citrate can be elucidated electrochemically. According to the literature [25], Tafel analysis can provide relevant aspects of electrochemical reactions. The well-known Tafel (Equation 3) and Tafel coefficient (Equation 4) relation can be used to resolve the reaction mechanism or even to determine the reaction determinant step (rds) of the electrochemical reaction.

$$\eta = a + \frac{2.303RT}{\alpha nF} log i_{corr} \quad (Eq. 3)$$

$$\frac{\partial \eta}{\partial log i_{corr}} = \frac{2.303RT}{\alpha nF} \quad (Eq. 4)$$

Where η is the overpotential, α is the Symmetry coefficient, and n is the exchange electron number.

In the cathodic region, we have the electrochemical evolution of gaseous hydrogen. Considering the value of the Tafel coefficient close to 118 mV/dec, we have reaction determinant step (rds) described by the Volmer pathway, such as in Equations 5 and 6 [26,27]. However, with a coefficient of around 60 mV/dec, step 2 is the most likely [27]. As can be seen from Figure 2, the coefficient of anodic Tafel without the addition of inhibitor has a value of 62 mV/dec. This Tafel coefficient is theoretically compatible with a chemical step (Tafel pathway such as equation 7) representing the slow step of the hydrogen evolution reaction. With the addition of the inhibitor, this value increases to 80 mV/dec. According to the literature, an increase in the Tafel coefficient can mean a variation in the α [25].

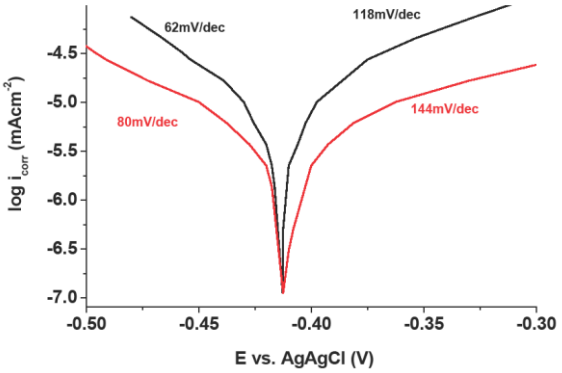

Figure 2. Tafel plot of carbon steel in pH = 6.00 and 125ppm of chloride, with and without the addition of Na_3Cit.

$$H^+_{(aq)} + e^- \rightarrow H_{ads} \quad (Eq. 5)$$

$$H^+_{(aq)} + e^- + H_{ads} \rightarrow H_{2(g)} \quad (\text{Eq. } 6)$$
$$H_{ads} + H_{ads} \rightarrow H_{2(g)} \quad (\text{Eq. } 7)$$

On the anodic side, the obtained Tafel coefficient is 118mV/dec. This coefficient appears consistent with rds related to the oxidation shown in Equation 8 [28], with a subsequent step represented by Equation 9. Similarly to what was discussed for the cathode part, a change in the charge transfer coefficient caused by the adsorption of the inhibitor can cause an increase in the Tafel coefficient, as shown in Figure 2.

$$Fe_{(s)} + OH^-_{(aq)} \rightarrow FeOH^+_{(aq)} + 2e^- \quad (\text{Eq. } 8)$$
$$FeOH^+_{(aq)} \rightarrow Fe^{2+}_{(aq)} + OH^-_{(aq)} \quad (\text{Eq. } 9)$$

Figure 3 shows the fraction of species originating from citrate in relation to the pH value. Using the acid constant values of citric acid in 298 K (K_{a1} = 7.4 x10^{-4}, K_{a2} = 1.7 x$10^{-5,}$ and K_{a3} = 7.4 x10^{-7}[10]), we can calculate the fraction of species originating from citrate in relation to the pH value.

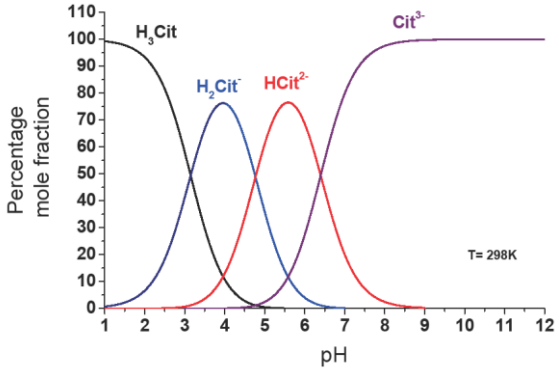

Figure 3. Fraction of species originating from citrate in relation to the pH.

For a polyprotic citric acid (H_3Cit), the equations that represent the percentage mole fraction of H_3Cit (β_1), H_2Cit^- (β_2), $HCit^{-2}$ (β_3), and Cit^{-3} (β_4), are respectively the Equations 10,11,12 and 13.

$$\beta_1 = \frac{100[H^+]}{[H^+] + [H^+]^2K_{a1} + [H^+]K_{a1}K_{a2} + K_{a1}K_{a2}K_{a3}} \quad (Eq. 10)$$
$$\beta_2 = \frac{100[H^+]^2K_{a1}}{[H^+] + [H^+]^2K_{a1} + [H^+]K_{a1}K_{a2} + K_{a1}K_{a2}K_{a3}} \quad (Eq. 11)$$
$$\beta_3 = \frac{100[H^+]K_{a1}K_{a2}}{[H^+] + [H^+]^2K_{a1} + [H^+]K_{a1}K_{a2} + K_{a1}K_{a2}K_{a3}} \quad (Eq. 12)$$
$$\beta_4 = \frac{100K_{a1}K_{a2}K_{a3}}{[H^+] + [H^+]^2K_{a1} + [H^+]K_{a1}K_{a2} + K_{a1}K_{a2}K_{a3}} \quad (Eq. 13)$$

The percentage of citrate species at pH = 6 is approximately 69% of $HCit^{-2}$, 6% of H_2Cit^- and 25% of Cit^{-3}. This complex distribution makes it difficult to analyze the anticorrosive effect of citrate in solution. A study using adsorption isotherms was carried out to discuss the inhibition of Na_3Cit through chemisorption or physisorption.

3.1. Adsorption isotherms and kinetic analysis.

Initially, the first step to inhibit corrosion begins with an adsorption of the inhibitor on the active surface of the metal. The Langmuir adsorption model considers that inhibitors adsorb

through a monolayer, where the adsorption enthalpy variation (ΔH_{ads}) does not change with the advancement of adsorption. Considering citrate anions (Na_3Cit) as a corrosion inhibitor, in this case, the Langmuir isotherm for adsorption is given by Equation 14.

$$\frac{[Na_3Cit]_{eq}}{\theta} = \frac{1}{k_{ads}} + [Na_3Cit]_{eq} \qquad \text{(Eq. 14)}$$

where K_{ads} is the adsorption constant

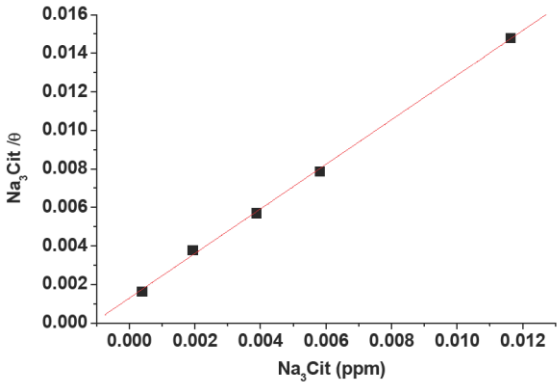

Figure 4. The linear fit of Languimir isotherm for carbon steel immersed in a solution at pH = 6.00 with different values of Na_3Cit concentration.

Figure 4 shows the linear fit using Equation 13 for carbon steel immersed in a solution at pH = 6.00 with different values of Na_3Cit concentration. The value of ΔG_{ads} can be obtained from k_{ads} (Equation 15).

$$k_{ads} = \left(\frac{1}{55.5}\right) e^{\frac{-\Delta Gads}{RT}} \qquad (Eq.15)$$

Where: R is the gas constant (8.3144621 $JK^{-1}mol^{-1}$); T is the temperature in Kelvin, and ΔG_{ads} is the Free Gibbs energy of adsorption.

Ea is the activation energy, T is the temperature in Kelvin, and A is the exponential factor.

According to the literature, values lower in modulus than -20 kJ/mol for energy adsorption are related to physisorption. On the other hand, values close to -40 kJ/mol are reported as chemisorption [5]. We see a mixed behavior in this case since the values are between 20 and 40 kJ/mol (table 1).

Table 1. Linear fit using the Langmuir isotherm for carbon steel immersed in a solution at pH = 6.00 and 125 ppm of Cl^- with different values of Na_3Cit concentration.

pH	K_{ads}	Angular coefficient	R^2	ΔG_{ads} (kJ/mol)
6.00	5.58 x10^3	1.15	0.999	-31,32

One can analyze the corrosion results with temperature variation using the transition state theory, which corresponds to an alternative approach to the Arrhenius formulation (16) [30-32]. This result is shown in Figure 5.

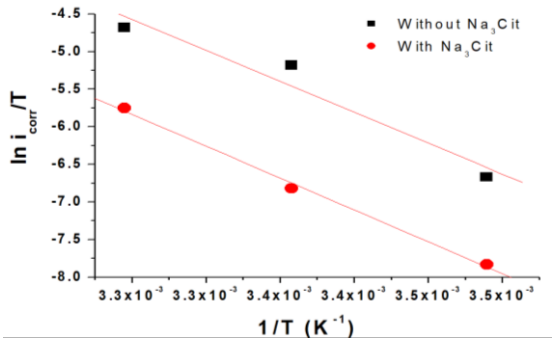

Figure 5. The Arrhenius plot for carbon steel in pH = 6.00 and 125ppm of chloride, with and without the addition of Na_3Cit.

$$ln\left(\frac{I_{corr}}{T}\right) = ln\frac{R}{Nh} - \frac{\Delta S^{\#}}{R} - \frac{\Delta H^{\#}}{RT} \qquad (Eq.16)$$

Where: **N**: Avogadro's number (6.02214179 x 10^{23}); **h**: Planck's constant; $\mathbf{\Delta H^{\#}}$ and $\mathbf{\Delta S^{\#}}$: are Enthalpy and Entropy variation for activated complex formation, respectively.

It is observed that, with inhibitor addition, the $\Delta H^{\#}$ value subtly decreases from 70.50 to 68.44 kJ/mol (Table 2). This feature shows that in the corrosion process, the adsorption of inhibitor molecules occurs mainly through chemisorption [30]. Several theories are used in the literature to explain this phenomenon. According to Riggs and Hurd [31], with high concentrations of inhibitors, the corrosion reaction shifts to covered regions of the electrode surface, which causes a decrease in the activation energy [30]. Based on the studies by Schmid and Huang [30], we propose the possibility that citric acid, formed at the electrified interface, can inhibit the cathodic and anodic reaction by changing the symmetry coefficient. According to the literature for the most negative entropy values, implications that the slow step of the reaction is more related to the formation of the activated complex rather than its dissociation [32]. Furthermore, the increased $\Delta G^{\#}$ value of 70.57 to 100.13 kJ/mol (Table 2) using the corrosion inhibitor shows that the process becomes less spontaneous for forming the activated complex.

Table 2. Linear fit using the Langmuir isotherm for carbon steel immersed in a solution at pH = 6.00 and 125ppm of Cl^- with different values of Na_3Cit concentration.

Inhibitor concentration in ppm	$\Delta H^{\#}$(kJ/mol)	$\Delta S^{\#}$(J/Kmol)	$\Delta G^{\#}$(kJ/mol)
0	70.50	-77.05	´70.57
3000	68.44	-106.37	100.13

3.2. X-ray diffraction and SEM and EDS.

Figure 6 shows the XDR measure of carbon steel after 2h in a 125ppm Cl^- solution at pH = 6, with and without the addition of Na_3Cit.

After corrosion, it is noted CCC (body-centered cubic), with crystallographic planes [110] and [200] at 44.93º and 65.49º, respectively, in both with and without Na_3Cit. In the sample without adding Na_3Cit, the corresponding peaks of the Fe_3O_4, β −FeOOH, and $FeCO_3$ phases are found. According to the literature, an β −FeOOH phase is strongly influenced by the presence of chloride ions. It is clearly noted that with the addition of Na_3Cit, the formation of the β −FeOOH phase is strongly suppressed. According to the literature [33], the formation of complexes with Fe^{+3} can influence the formation of the β −FeOOH phase.

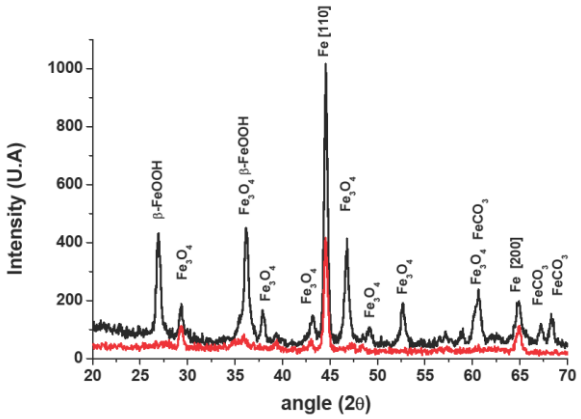

Figure 6. XDR measure of carbon steel after 2 h in a 125ppm Cl^- solution at pH = 6, with and without the addition of Na_3Cit.

Moreover, for a steel sample that was immersed in the citrate solution, a clear reduction in the intensity of the peaks in the diffractogram can be noted. This reduction is due to the smaller amount of corrosion product formed as a result of the decrease in the corrosion rate caused by citrate inhibition.

Figure 7 shows the SEM of carbon steel after 2 h in a 125 ppm Cl^- solution at pH = 6, with and without the addition of Na_3Cit.

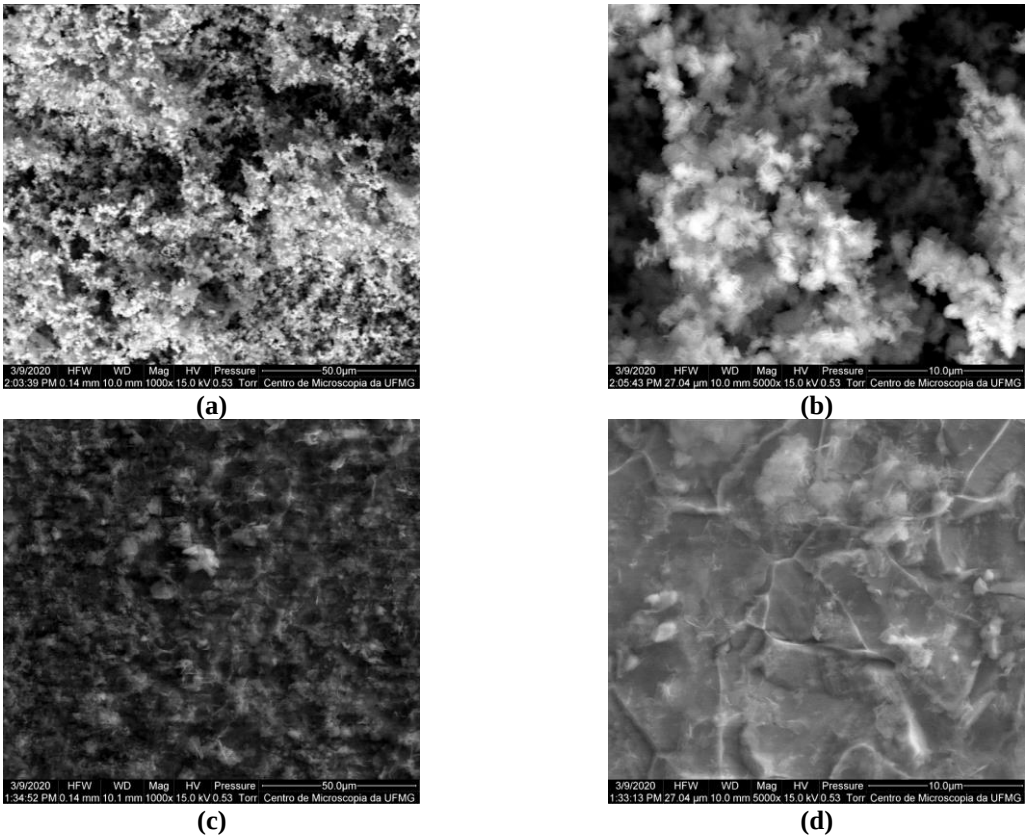

(a) **(b)** **(c)** **(d)**

Figure 7. SEM of carbon steel after 2h in a 125ppm Cl^- solution at pH = 6: **(a)** with the addition of Na_3Cit, in 50 µm; **(b)** with the addition of Na_3Cit, in 10 µm; **(c)** without the addition of Na_3Cit, in 50 µm; **(d)** without the addition of Na_3Cit, in 10 µm.

There is a clear difference between the sample with and without the corrosion inhibitor (Figure 7). In the sample without the inhibitor, a typical surface of a corrosion process is presented, with an irregular surface due to the action of cathode and anode sites. On the other

hand, from the sample with the corrosion inhibitor, a surface presents more smoothly due to a possible formation of a tiny film not detectable by SEM [34].

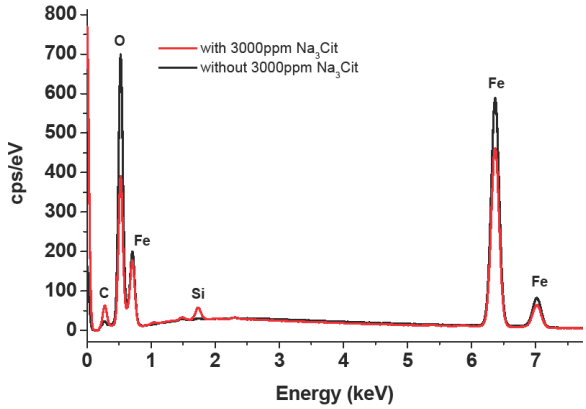

Figure 8. EDX of carbon steel after 2h in a 125ppm Cl^- solution at pH = 6, with and without the addition of Na_3Cit.

The chemical composition of the surface was also studied using the EDX measures (Figure 8). It is noted that the amount of oxygen on the sample's surface is significantly less in the sample with the corrosion inhibitor. Moreover, the amount of surface carbon increases in the sample with the inhibitor. This could be an indication of an inhibitor film adhered to the surface due to the chemisorption process.

4. Conclusions

The Na_3Cit promotes a reduction of around 80% of the corrosion rate of carbon steel at 125ppm Cl- at pH =6. In the anodic region, the Tafel coefficient is theoretically compatible with the Tafel pathway for hydrogen evolution. On the anodic side, the obtained Tafel coefficient is compatible with a mechanism that passes through an intermediary $FeOH^+_{(aq)}$. In both cases, the presence of the inhibitor caused an increase in the Tafel coefficient, possibly due to the change in the alpha value. According to adsorption measurements, the carbon steel inhibition process in citrate can be characterized as a mixture of chemisorption and physisorption. Thermodynamic values for the activated complex also indicate a mixed mechanism. Furthermore, the increase in $\Delta G^{\#}$ value shows that the corrosion process is less spontaneous when using Na_3Cit as a corrosion inhibitor. Through XRD measurements for a steel sample immersed in the citrate solution, there is a clear reduction in the intensity of the peaks in the diffractogram due to the smaller amount of corrosion product formed. Furthermore, EDX and SEM measurements corroborate the formation of a thin inhibitor layer on the steel.

Funding

This research received no external funding.

Acknowledgments

The authors would like to thank authors thank the Brazilian agencies CNPq, FAPEMIG, CAPES, and Rede Mineira de Química (RQ-MG) for their support.

Conflicts of Interest

The authors declare no conflict of interest.

References

1. Serdaroğlu, G.; Kaya, S.; Touir, R. Eco-friendly sodium gluconate and trisodium citrate inhibitors for low carbon steel in simulated cooling water system: Theoretical study and molecular dynamic simulations. *J. Mol. Liq* **2020**, *319*, 114108, https://doi.org/10.1016/j.molliq.2020.114108.
2. Liu, Y.; Shi, J. Corrosion resistance of carbon steel in alkaline concrete pore solutions containing phytate and chloride ions. *Corros. Sci.* **2022**, *205*, 110451, https://doi.org/10.1016/j.corsci.2022.110451.
3. Wu, S.; Wang, J.; Liu, T.; Guo, X.; Ma, L. Sulfosalicylic acid modified carbon dots as effective corrosion inhibitor and fluorescent corrosion indicator for carbon steel in HCl solution. *Colloids Surf. A: Physicochem. Eng. Asp.* **2023**, *661*, 130951, https://doi.org/10.1016/j.colsurfa.2023.130951.
4. Park, J.-H.; Hagio, T.; Ichino, R. Improvement in the corrosion resistance of electrodeposited Ni-W alloy by MWCNT co-deposition and prevention of metal-carbon interfacial corrosion by carbide formation. *J. Alloys Compd.* **2023**, *939*, 168788, https://doi.org/10.1016/j.jallcom.2023.168788.
5. Semedo, R.A.R.; Alcanfor, A.A.C.; Sousa, N.G.; Casciano, P.N.S.; Correia, A.N.; Pereira, J.C.; de Lima-Neto, P. Evaluation of corrosion resistance of Zn_x-Mn_{1-x} coatings electrodeposited on 1020 carbon steel rotating electrode from choline chloride and urea at eutectic composition. *Mater. Chem. Phys.* **2023**, *307*, 128074, https://doi.org/10.1016/j.matchemphys.2023.128074.
6. Marunkić, D.; Jegdić, B.; Pejić, J.; Milošević, M.; Marinković, A.; Radojkovć, B. Analysis of inhibitory properties of Ce-citrate as a green corrosion inhibitor of low alloy steel in neutral chloride solution. *Mater. Corros.* **2022**, *73*, 1286-1297, https://doi.org/10.1002/maco.202213079.
7. Marunkić, D.; Pejić, J.; Jegdić, B.; Marinković, A.; Radojković, B. Cerium citrate as ecologically friendly corrosion inhibitor for AA7075 alloy. *Mater. Corros.* **2022**, *73*, 950-960, https://doi.org/10.1002/maco.202112900.
8. Maciej, S.; Aleksander, O.; Bartosz, S.; Artur, M.; Maciej, B.; Piotr, J.; Maciej, S.; Wojciech, S. Electrochemical characterization of anti-corrosion coatings formed on 6061 aluminum alloy by plasma electrolytic oxidation in the corrosion inhibitor-enriched aqueous solutions. *Electrochim. Acta*. **2022,** 424, 140652, https://doi.org/10.1016/j.electacta.2022.140652.
9. Zhang, X.; Tan, B.; Li, W. Chapter16 - Plant extracts as environmentally sustainable corrosion inhibitors I. In Eco-Friendly Corrosion Inhibitors, Guo, L., Verma, C., Zhang, D., Eds.; Elsevier, **2022**; 263-282, https://doi.org/10.1016/B978-0-323-91176-4.00011-8.
10. Berdimurodov, E.; Kholikov, A.; Akbarov, K.; Guo, L.; Umirov, N.; Verma, D. K.; Rbaa, M.; Dagdag, O.; Haldhar, R.; Kaya, S. Ionic liquids as green and sustainable corrosion inhibitors I. *Eco-Friendly Corrosion inhibitor*. **2022**, 331-390, https://doi.org/10.1016/B978-0-323-91176-4.00020-9.
11. Guo, L.; Verma, C.; Zhang, D. Eco-Friendly Corrosion Inhibitor: Principles, Designing and Aplications, 1st Edition; Elsevier, **2022**, https://doi.org/10.1016/C2020-0-04557-3.
12. Behera, B.C.; Mishra, R.; Mohapatra, S. Microbial citric acid: Production, properties, application, and future perspectives. *Food Front.* **2021**, *2*, 62-76, https://doi.org/10.1002/fft2.66.
13. Wang, F.; Zou, Z.-S.; He, Z.-W.; Tang, C.-C.; Zhou, A.-J.; Liu, W.; Ren, Y.-X.; Li, Z.; Wang, A. Revealing methane production potential from waste activated sludge through citric acid-assisted hydrogen corrosion of zero valent iron. *Chem. Eng. J.* **2023**, *473*, 145195, https://doi.org/10.1016/j.cej.2023.145195.
14. Tan, J.K.E.; Birbilis, N.; Choudhary, S.; Thomas, S.; Balan, P. Corrosion protection enhancement of Mg alloy WE43 by in-situ synthesis of MgFe LDH/citric acid composite coating intercalated with 8HQ. *Corros. Sci.* **2022**, *205*, 110444, https://doi.org/10.1016/j.corsci.2022.110444.
15. Li, X.; Deng, S. $Ce(SO_4)_2$ as an efficient corrosion inhibitor for cold rolled steel in citric acid solution. *J. Taiwan Inst. Chem. Eng.* **2021**, *122*, 273-283, https://doi.org/10.1016/j.jtice.2021.04.057.
16. Ouarga, A.; Zirari, T.; Fashu, S.; Lahcini, M.; Youcef, H.B.; Trabadelo, V. Corrosion of iron and nickel based alloys in sulphuric acid: Challenges and prevention strategies. *J. Mater. Res. Technol.* **2023**, *26*, 5105-5125, https://doi.org/10.1016/j.jmrt.2023.08.198.
17. Jeeja, R.A.T.; Kuruvilla, M.; Joseph, A. Computational modelling and theoretical calculations on hydroxy citric acid and mangostine and comparing the corrosion inhibition effect of aqueous and alcoholic extracts

Garcinia cambogia leaves for mild steel in hydrochloric acid. *J. Mol. Struct.* **2023**, *1274*, 134302, https://doi.org/10.1016/j.molstruc.2022.134302.
18. Zhang, X.; Su, Y.; Zhang, Y.; Guan, S.; Wang, X.; He, Y. A quinoline-based quaternary ammonium salt dimer as corrosion inhibitor for N80 steel in lactic acid solution. *J. Mol. Struct.* **2023**, *1290*, 135914, https://doi.org/10.1016/j.molstruc.2023.135914.
19. Odunlami, O.A.; Loto, R.T.; Fajobi, M.A.; Olomukoro, O.T.; Akande, I.G.; Oke, M.A.; Oladimeji, T.E. Data on the corrosion Inhibition Property of Rosemary on High Carbon Steel in dilute sulphuric acid, citric acid and sodium chloride solution. *Chem. Data Collect.* **2021**, *32*, 100660, https://doi.org/10.1016/j.cdc.2021.100660.
20. Zhu, M.; He, Z.; Guo, L.; Zhang, R.; Anadebe, V.C.; Obot, I.B.; Zheng, X. Corrosion inhibition of eco-friendly nitrogen-doped carbon dots for carbon steel in acidic media: Performance and mechanism investigation. *J. Mol. Liq.* **2021**, *342*, 117583, https://doi.org/10.1016/j.molliq.2021.117583.
21. Fernández-Domene, R.M.; Roselló-Márquez, G.; Sánchez-Tovar, R.; Cifre-Herrando, M.; García-Antón, J. Synthesis of WO_3 nanorods through anodization in the presence of citric acid: Formation mechanism, properties and photoelectrocatalytic performance. *Surf. Coat. Technol.* **2021**, *422*, 127489, https://doi.org/10.1016/j.surfcoat.2021.127489.
22. Modiano, S.; Fugivara, C.S.; Benedetti, A.V. Effect of citrate ions on the electrochemical behavior of low carbon steel in borate buffer solutions. *Corros. Sci.* **2004**, *46*, 529-545, https://doi.org/10.1016/S0010-938X(03)00170-7.
23. Diab, A.; Abd El-Haleem, S.M. Inhibition Effect of Some Organic Compounds Toward the Corrosion of Steel Electrode in Citric Acid Solution Infected by Way of Chloride Ions. *Orient. J. Chem.* **2017**, *33*, 1921, http://dx.doi.org/10.13005/ojc/330438.
24. Ashassi-Sorkhabi, H.; Asghari, E.; Mohammadi, M. Effects of Solution Hydrodynamics on Corrosion Inhibition of Steel by Citric Acid in Cooling Water. *J. Mater. Eng. Perform.* **2014**, *23*, 2992–3000, https://doi.org/10.1007/s11665-014-1047-z.
25. Santos, D.M.F.; Sequeira, C.A.C.; Macciò, D.; Saccone, A.; Figueiredo, J.L. Platinum-rare earth electrodes for hydrogen evolution in alkaline water electrolysis. *Int. J. Hydrog. Energy* **2013**, *38*, 3137-3145, https://doi.org/10.1016/j.ijhydene.2012.12.102.
26. Tian, J.; Wu, W.; Tang, Z.; Wu, Y.; Burns, R.; Tichnell, B.; Liu, Z.; Chen, S. Oxygen Reduction Reaction and Hydrogen Evolution Reaction Catalyzed by Pd–Ru Nanoparticles Encapsulated in Porous Carbon Nanosheets. *Catalysts* **2018**, *8*, 329, http://dx.doi.org/10.3390/catal8080329.
27. Pentland, N.; Bockris, J.O'M.; Sheldon, E. Hydrogen Evolution Reaction on Copper, Gold, Molybdenum, Palladium, Rhodium, and Iron: Mechanism and Measurement Technique under High Purity Conditions. *J. Electrochem. Soc.* **1957**, *104*, 182, https://doi.org/10.1149/1.2428530.
28. Bockris, J.O'M.; Drazic, D.; Despic, A.R. The electrode kinetics of the deposition and dissolution of iron. *Electrochim. Acta* **1961**, *4*, 325-361, https://doi.org/10.1016/0013-4686(61)80026-1.
29. Elbagermi, M.A.; Alajtal, A.I.; Edwards, H.G.M.; Azimi, G.H.; Verma, K.D.; Scowen, I.J. RAMAN SPECTROSCOPIC AND POTENTIOMETRIC STUDIES OF ACIDITY LEVEL AND DISSOCIATION OF CITRIC ACID IN AQUEOUS SOLUTION. *J. Appl. Chem. Sci. Int.* **2015**, *2*, 1-11.
30. Schmid, G.M.; Huang, H.J. Spectro-electrochemical studies of the inhibition effect of 4,7-diphenyl-1, 10-phenanthroline on the corrosion of 304 stainless steel. *Corros. Sci.* **1980**, *20*, 1041-1057, https://doi.org/10.1016/0010-938X(80)90083-9.
31. Riggs Jr., O.L.; Hurd, R.M. Temperature Coefficient of Corrosion Inhibition. *Corrosion* **1967**, *23*, 252-260, https://doi.org/10.5006/0010-9312-23.8.252.
32. Go, L.C.; Depan, D.; Holmes, W.E.; Gallo, A.; Knierim, K.; Bertrand, T.; Hernandez, R. Kinetic and thermodynamic analyses of the corrosion inhibition of synthetic extracellular polymeric substances. *PeerJ Mater. Sci.* **2020**, *2*, e4, https://doi.org/10.7717/peerj-matsci.4.
33. Song, Y.; Jiang, G.; Chen, Y.; Zhao, P.; Tian, Y. Efects of chloride ions on corrosion of ductile iron and carbon steel in soil environments. *Sci. Rep.* **2017**, *7*, 6865, https://doi.org/10.1038/s41598-017-07245-1.
34. Mahdavian, M.; Attar, M.M. Electrochemical behaviour of some transition metal acetylacetonate complexes as corrosion inhibitors for mild steel. *Corros. Sci.* **2009**, *51*, 409-414, https://doi.org/10.1016/j.corsci.2008.11.010.